# Highly-photostable and mechanically flexible all-organic semiconductor lasers

**C. Foucher,[1,*] B. Guilhabert,[1] A. L. Kanibolotsky,[2] P. J. Skabara,[2] N. Laurand,[1] and M. D. Dawson[1]**

[1]*Institute of Photonics, University of Strathclyde, Glasgow G4 0NW, UK*
[2]*WestCHEM, Pure and Applied Chemistry Department, University of Strathclyde, Glasgow G1 1XL, UK*
**caroline.foucher@strath.ac.uk*

**Abstract:** Two formats of all-organic distributed-feedback lasers with improved photostability, respectively called nanocomposite and encapsulated lasers, are reported. These lasers are compatible with mechanically-flexible platforms and were entirely fabricated using soft-lithography and spin-coating techniques. The gain elements in both types of lasers were monodisperse π-conjugated star-shaped macromolecules (oligofluorene truxene, T3). In the nanocomposites lasers, these elements were incorporated into a transparent polyimide matrix, while in the encapsulated devices a neat layer of T3 was overcoated with Poly(vinyl alcohol) (PVA). The T3-nanocomposite devices demonstrated a 1/e degradation energy dosage up to ~27.0 ± 6.5 J/cm$^2$ with a threshold fluence of 115 ± 10 μJ/cm$^2$. This represents a 3-fold improvement in operation lifetime under ambient conditions compared to the equivalent laser made with neat organic films, albeit with a 1.6-time increase in threshold. The PVA-encapsulated lasers showed the best overall performance: a 40-time improvement in the operation lifetime and crucially no-trade-off on the threshold, with respectively a degradation energy dosage of ~280 ± 20 J/cm$^2$ and a threshold fluence of 36 ± 8 μJ/cm$^2$.



**OCIS codes**: (140.3460) Lasers; (160.4890) Organic materials.

## References and links

1. I. D. W. Samuel and G. A. Turnbull, "Organic semiconductor lasers," Chem. Rev. **107**(4), 1272–1295 (2007).
2. P. Görrn, M. Lehnhardt, W. Kowalsky, T. Riedl, and S. Wagner, "Elastically tunable self-organized organic lasers," Adv. Mater. **23**(7), 869–872 (2011).
3. B. Wenger, N. Tétreault, M. E. Welland, and R. H. Friend, "Mechanically tunable conjugated polymer distributed feedback lasers," Appl. Phys. Lett. **97**(19), 193303 (2010).
4. S. Riechel, U. Lemmer, J. Feldmann, T. Benstem, W. Kowalsky, U. Scherf, A. Gombert, and V. Wittwer, "Laser modes in organic solid-state distributed feedback lasers," Appl. Phys. B **71**(6), 897–900 (2000).
5. K. Suzuki, K. Takahashi, Y. Seida, K. Shimizu, M. Kumagai, and Y. Taniguchi, "A continuously tunable organic solid-state laser based on a flexible distributed-feedback resonator," Jpn. J. Appl. Phys. **42**(Part 2, No. 3A), L249–L251 (2003).
6. M. R. Weinberger, G. Langer, A. Pogantsch, A. Haase, E. Zojer, and W. Kern, "Continuously color-tunable rubber laser," Adv. Mater. **16**(2), 130–133 (2004).
7. B. Guilhabert, D. Massoubre, E. Richardson, J. J. D. McKendry, G. Valentine, R. K. Henderson, I. M. Watson, E. Gu, and M. D. Dawson, "Sub-micron lithography using InGaN micro-LEDs: mask-free fabrication of LED arrays," IEEE Photon. Technol. Lett. **24**(24), 2221–2224 (2012).
8. J. Herrnsdorf, B. Guilhabert, Y. Chen, A. Kanibolotsky, A. Mackintosh, R. Pethrick, P. Skabara, E. Gu, N. Laurand, and M. Dawson, "Flexible blue-emitting encapsulated organic semiconductor DFB laser," Opt. Express **18**(25), 25535–25545 (2010).
9. S. Klinkhammer, N. Heussner, K. Huska, T. Bocksrocker, F. Geislhöringer, C. Vannahme, T. Mappes, and U. Lemmer, "Voltage-controlled tuning of an organic semiconductor distributed feedback laser using liquid crystals," Appl. Phys. Lett. **99**(2), 023307 (2011).
10. A. Camposeo, P. Del Carro, L. Persano, and D. Pisignano, "Electrically tunable organic distributed feedback lasers embedding nonlinear optical molecules," Adv. Mater. **24**(35), OP221–OP225 (2012).

#186104 - $15.00 USD Received 4 Mar 2013; revised 2 Apr 2013; accepted 2 Apr 2013; published 10 Apr 2013

11. M. H. Song, B. Wenger, and R. H. Friend, "Tuning the wavelength of lasing emission in organic semiconducting laser by the orientation of liquid crystalline conjugated polymer," Appl. Phys. Lett. **104**(3), 033107 (2008).
12. S. Chénais and S. Forget, "Recent advances in solid-state organic lasers," Polym. Int. **61**(3), 390–406 (2012).
13. Y. Yang, G. A. Turnbull, and I. D. W. Samuel, "Hybrid optoelectronics: a polymer laser pumped by a nitride light-emitting diode," Appl. Phys. Lett. **92**(16), 163306 (2008).
14. T. Riedl, T. Rabe, H.-H. Johannes, W. Kowalsky, J. Wang, T. Weimann, P. Hinze, B. Nehls, T. Farrell, and U. Scherf, "Tunable organic thin-film laser pumped by an inorganic violet diode laser," Appl. Phys. Lett. **88**(24), 241116 (2006).
15. A. E. Vasdekis, G. Tsiminis, J. C. Ribierre, L. O' Faolain, T. F. Krauss, G. A. Turnbull, and I. D. Samuel, "Diode pumped distributed Bragg reflector lasers based on a dye-to-polymer energy transfer blend," Opt. Express **14**(20), 9211–9216 (2006).
16. N. Grassie, and G. Scott, *Polymer Degradation and Stabilisation* (Cambridge University Press, 1985).
17. W. Zhao, T. Cao, and J. M. White, "On the origin of green emission in polyfluorene polymers: the roles of thermal oxidation degradation and crosslinking," Adv. Funct. Mater. **14**(8), 783–790 (2004).
18. L. Cerdán, A. Costela, G. Durán-Sampedro, I. García-Moreno, M. Calle, M. Juan-y-Seva, J. de Abajo, and G. A. Turnbull, "New perylene-doped polymeric thin films for efficient and long-lasting lasers," J. Mater. Chem. **22**(18), 8938–8947 (2012).
19. S. Richardson, O. P. M. Gaudin, G. A. Turnbull, and I. D. W. Samuel, "Improved operational lifetime of semiconducting polymer lasers by encapsulation," Appl. Phys. Lett. **91**(26), 261104 (2007).
20. J. Buseman-Williams, K. D. Frischknecht, M. D. Hubert, A. K. Saafir, and J. D. Tremel, "Flat-plate encapsulation solution for OLED displays using a printed getter," J. Soc. Inf. Disp. **15**(2), 103–112 (2007).
21. A. L. Kanibolotsky, R. Berridge, P. J. Skabara, I. F. Perepichka, D. D. Bradley, and M. Koeberg, "Synthesis and properties of monodisperse oligofluorene-functionalized truxenes: highly fluorescent star-shaped architectures," J. Am. Chem. Soc. **126**(42), 13695–13702 (2004).
22. G. Tsiminis, Y. Wang, P. E. Shaw, A. L. Kanibolotsky, I. F. Perepichka, M. D. Dawson, P. J. Skabara, G. A. Turnbull, and I. D. W. Samuel, "Low-threshold organic laser based on an oligofluorene truxene with low optical losses," Appl. Phys. Lett. **94**(24), 243304 (2009).
23. http://www.mantechmaterials.com/products.asp.
24. L. Cerdán, A. Costela, I. García-Moreno, O. García, R. Sastre, M. Calle, D. Muñoz, and J. de Abajo, "High-gain long-lived amplified spontaneous emission from dye-doped fluorinated polyimide planar waveguides," Macromol. Chem. Phys. **210**(19), 1624–1631 (2009).
25. J. G. Pritchard, *Poly (vinyl alcohol): Basic Properties and Uses* (Gordon and Breach, 1970).
26. P. V. Adhyapak, N. Singh, A. Vijayan, R. C. Aiyer, and P. K. Khanna, "Single mode waveguide properties of m-NA doped Au/PVA nano-composites: synthesis, characterization and studies," Mater. Lett. **61**(16), 3456–3461 (2007).
27. M. M. W. Muscatello and S. A. Asher, "Poly (vinyl alcohol) rehydratable photonic crystal sensor materials," Adv. Funct. Mater. **18**(8), 1186–1193 (2008).
28. Q. Bao and K. P. Loh, "Graphene photonics, plasmonics, and broadband optoelectronic devices," ACS Nano **6**(5), 3677–3694 (2012).
29. O. G. Abdullah and D. R. Saber, "Optical absorption of polyvinyl alcohol films doped with nickel chloride," Appl. Mech. Mater. **110-116**, 177–182 (2011).
30. J. Gaume, P. Wong-Wah-Chung, A. Rivaton, S. Thérias, and J.-L. Gardette, "Photochemical behavior of PVA as an oxygen-barrier polymer for solar cell encapsulation," RSC Adv. **1**(8), 1471–1481 (2011).
31. J. Brandrup, E. H. Immergut, and E. A. Grulke, *Polymer Handbook* (Wiley, 1999).
32. J. Chilwell and I. Hodgkinson, "Thin-films field-transfer matrix theory of planar multilayer waveguides and reflection from prism-loaded waveguides," J. Opt. Soc. Am. **1**(7), 742–753 (1984).
33. S. Riechel, U. Lemmer, J. Feldmann, S. Berleb, A. G. Mückl, W. Brütting, A. Gombert, and V. Wittwer, "Very compact tunable solid-state laser utilizing a thin-film organic semiconductor," Opt. Lett. **26**(9), 593–595 (2001).
34. M. Lu, B. T. Cunningham, S.-J. Park, and J. G. Eden, "Vertically emitting, dye-doped polymer laser in the green (λ ~536 nm) with a second order distributed feedback grating fabricated by replica molding," Opt. Commun. **281**(11), 3159–3162 (2008).

## 1. Introduction

Organic semiconductors (OS) are promising materials for the fabrication of photonic devices as they can be tailored to emit across the whole visible spectrum and exhibit high photoluminescence quantum yield [1]. They also benefit from potential low production cost and toxicity while their 'soft matter' nature offers great processing flexibility, enabling for example a wide range of novel bendable and mechanically-tunable devices such as OS lasers [2–8]. Wavelength electrical-tuning of OS lasers has also been shown [9–11]. Consequently, research on easy-to-fabricate and potentially disposable OS lasers based on these materials is being keenly pursued [12]. However, as there has still been no report of electrically-injected

#186104 - $15.00 USD Received 4 Mar 2013; revised 2 Apr 2013; accepted 2 Apr 2013; published 10 Apr 2013

OS lasers, pulsed optical pumping is seen as the practical solution to implementation, motivating the recent demonstrations of laser diode and LED-pumped OS lasers [13–15].

One critical issue which has limited the application of OS lasers in 'real-world' settings so far is that OS degrade under operation in an uncontrolled environment. The main mechanisms responsible for such degradation are heat, which can engender thermal decomposition, and photo-oxidation [16–18]. For practical applications, it is critical to mitigate these issues by (i) minimising heat build-up in OS through an increase in thermal conductivity and/or possibly low-repetition rate operation and by (ii) preventing photo-oxidation through isolation of the OS gain materials from the environment. One possible way to achieve this is to embed the OS emitters within an appropriate polymeric host matrix, creating (when the OS gain molecules are of appropriate size) a nanocomposite. OS lasers have been reported using such an approach, showing extended photostability but to the detriment of the laser threshold performance [8,19]. Another way to improve the lifetime of an organic laser is to 'encapsulate', i.e. to overcoat, the OS with another material acting as an oxygen barrier. However, for mechanically-flexible lasers it is also necessary to maintain the overall mechanical properties of the device. Therefore, standard encapsulation techniques making use of thick inorganic materials such as often used in OLED technology are not directly applicable here [20].

In this study, we demonstrate all-organic, one dimensional, second-order distributed feedback (DFB) lasers with improved photo-stability based on, respectively, a nanocomposite and an encapsulated gain region, that are both compatible with the fabrication of mechanically-flexible devices. In the following, section 2 explains the design and fabrication of these flexible lasers including the choice of the different materials. In section 3, the optical set-up used for their characterisation is detailed and the multilayer slab waveguide model, whose output is utilised in the discussion of the experimental results of section 4, is presented. Finally, section 4 discusses the experimental results for the nanocomposite lasers and the encapsulated lasers. The photostability in air of each type is measured and compared with reference lasers made with neat OS (based on a pure film of OS, i.e. not incorporated in a matrix nor encapsulated) in order to identify the best performing structure with both low lasing threshold and high photostability. In addition, as one of the possible applications of the neat and nanocomposite OS lasers is bio-sensing, which typically necessitates operation in polar solvents, e.g. biological buffers, the photostability of these devices when immersed in deionised water is also reported when applicable.

## 2. Design and fabrication

### *2.1. Structure of the mechanically-flexible lasers*

Figures 1 (a), 1(b) and 1(c) show the structures of the three types of lasers studied in this work, namely neat, nanocomposite and encapsulated lasers. They are all formed by a gain layer deposited on top of a one-dimensional, mechanically-flexible grating acting as a distributed feedback (DFB) reflector. The gain layer of both neat and encapsulated lasers is made of pure OS whereas the OS is incorporated into a transparent polyimide matrix in the case of the nanocomposite lasers. Encapsulated lasers are further overcoated with a protective layer of poly(vinyl alcohol) (PVA). Common to all these lasers, the active element of the gain layer is a star-shaped tris(terfluorenyl) based on a truxene core (T3), an oligomer whose main luminescence is in the blue region of the visible spectrum. The synthesis of these monodispersed macromolecules is 100% reproducible [21] and they can form amorphous films with low-optical loss that are ideal for laser applications [22]. The gain spectrum of T3 spans the 410-450nm region while the absorption peaks at 375 nm.

The mechanically flexible grating is identical for all three types of laser. It is made by soft lithography using a glass master grating of an appropriate period (276 nm in this case) and with a typical modulation depth of 50 nm. The master grating is reproduced with an

#186104 - $15.00 USD Received 4 Mar 2013; revised 2 Apr 2013; accepted 2 Apr 2013; published 10 Apr 2013

ultraviolet-transparent and photo-curable epoxy material, Norland NOA65, which has a refractive index n~1.53 at 450 nm, a viscosity of 1200 cps at 25°C and an elasticity of 20,000 psi. A 0.1-mm-thick sheet of acetate is used as a substrate and pressed onto the master grating covered by epoxy. After photocuring under a UV dose of 300 mJ/cm$^2$ and wavelength of 370 nm, the flexible grating is peeled off the master and then further post-cured under UV for about an hour (~1.8 J/cm$^2$). A flexible grating replicating the features of the master is then obtained. An atomic force microscopy (AFM) image and a profile scan of a typical grating fabricated this way can be found in [7]. Further fabrication details specific to each type of lasers are given in the following sub-sections.

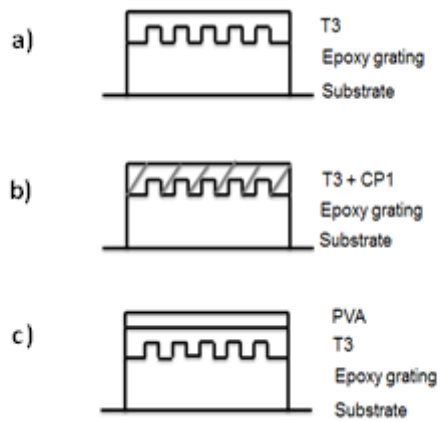


Fig. 1. Schematics of the device structures are shown: (a) neat T3 laser, (b) nanocomposite laser and (c) encapsulated laser.

*2.2. Neat T3 lasers*

For neat lasers, a layer of pure T3 is spin-coated onto the grating. At 430 nm, the refractive index of a typical spin-coated film is about 1.83 which ensures good confinement of the propagating mode within a waveguide structure. For processing, T3 in solid phase (powder) is dissolved in toluene, at a concentration of 20 mg/mL. To form OS lasers, the dispersed T3 is then spin-coated to form a film of ~75 ± 5 nm onto a mechanically-flexible grating and left to dry for a few minutes in air. Such a thickness, determined by controlling the spinning speed at deposition, ensures laser oscillation on a single TE-polarised mode.

A device was also made using tetrahydrofuran (THF) instead of toluene in order to verify the effect of the solvent on the operation lifetime of neat lasers and also because THF was utilised in the fabrication of nanocomposites lasers.

*2.3. Nanocomposite lasers*

For nanocomposite lasers, the choice of the matrix material is evidently important. Polyimides form a family of polymers that has some attractive attributes for playing that role (high glass temperature transition, TG, and resistance to harsh environmental conditions) but their lack of transparency in the visible has up to now logically forbidden their use in visible lasers. However, polyimides with improved transparency have recently been developed, now making them relevant [17,23,24]. A commercially-available fluorinated polyimide from Mantech, CP1, is used here as host matrix [23]. It offers low moisture permeability and has a TG of 263°C. It is transparent in the visible and has a 50% transparency cut-off at 409 nm for a 1mm-thick film, from data given in the material datasheet [23]. Its refractive index at 549 nm is specified at 1.57. It is expected that this material will facilitate heat transfer out of the OS [24] and reduce the oxygen permeability of the gain region to a certain extent, thereby improving the useful laser operating lifetime.

#186104 - $15.00 USD Received 4 Mar 2013; revised 2 Apr 2013; accepted 2 Apr 2013; published 10 Apr 2013

CP1 powder was dissolved in THF and T3 was directly added and dispersed inside the liquid matrix to the desired load of 4% wr CP1/T3 without addition of extra solvent. To choose this CP1 concentration, the amplified spontaneous emission of nanocomposites films having different ratios of CP1/T3 was measured (data not shown).

The refractive index of the nanocomposite material is estimated to be ~1.82 at 430 nm. The nanocomposite was spin-coated to form a film 75 ± 10 nm thick onto the mechanically-flexible grating. Again this thickness and refractive index values ensure that sufficient confinement is achieved to promote oscillation on the fundamental TE-polarised mode.

### *2.4. Encapsulated laser*

Poly (vinyl alcohol) (C2H4O)n, or PVA, was used in the fabrication of the encapsulated lasers. PVA is a highly transparent, water soluble polymer that has found many industrial applications, e.g. in food packaging, fishing nets and sail technology [25] but also in biomedicine and photonics. Recently, it has been used for the fabrication of optical waveguides [26], photonic crystal sensors [27] and as a host matrix for composites [28]. It is also seen as a good candidate for encapsulation of photonic devices because of its low oxygen permeability. For example it has been proposed for incorporation into multilayer coatings aimed at protecting organic solar cells from oxidation [29,30]. At 23°C PVA has an oxygen permeability coefficient of 5.0 x 10-17 $cm^3$ cm/($cm^2$.s.Pa) which compares very well to other transparent polymers: PET, another oxygen barrier polymer used in food packaging, has a coefficient of 3.1 x 10-15 $cm^3$ cm/($cm^2$ s Pa) [30,31]. Due to this low oxygen permeability, oxidation of PVA films tends to occur mostly at the interface with air. Products from photo-oxidation stay within 5 µm of this interface and do not affect the deeper layers of the material [30].

Similarly to the neat laser, T3 was dissolved in toluene at a concentration of 20 mg/mL and spin-coated on the grating to form a 75 ± 5 nm thick gain material layer. The film of PVA was prepared by mixing an 89% hydrolysed PVA powder, having a molecular weight in the range of 85,000-124,000 g/mol, with deionised (DI) water to obtain a concentration of 50 mg/ml. The solution was stirred for an hour at a temperature of 80°C. After being completely dissolved, the resulting solution was spin-coated on top of the T3 laser to form a film 180 ± 20 nm thick, measured by AFM. While a sub-micron PVA film might not totally suppress photo-oxidation of OS, it is still expected to slow down the process. The device was then annealed in air for three days at 35°C in order to totally evaporate the solvent and obtain a good crystalline cohesion [10].

Encapsulated lasers were also made using the same fabrication process but with a higher concentration (70 mg/mL) of PVA in order to achieve a thicker film (580 ± 70 nm). These lasers were used to check the influence the thickness of PVA has on the degradation behaviour of the lasers.

## 3. Photo-pumping experiments and model for mode profile calculations

### *3.1. Optical pumping*

The DFB lasers were optically pumped for characterisation by a Q-switched, frequency-tripled Nd:YAG laser emitting 5ns pulses at a wavelength of 355 nm and with a 10Hz repetition rate. The emission of a device was detected by a 50µm-core optical fibre, connected to a CCD-spectrometer with a maximum spectral resolution of 0.13 nm [8]. The samples were placed at an angle of about 45° with respect to the beam axis. The full width at half maximum (FWHM) pump spot size on the sample was 70,000 µm2 ± 5% for the nanocomposites lasers and 145,000 µm2 ± 5% for the encapsulated lasers, values measured by knife edge. The differing sizes of the pump spot are due to changes in the configuration of the system between both sets of measurements. However, it was verified that this difference had no significant effect on our lasers in terms of performance by measuring neat T3 lasers in

#186104 - $15.00 USD Received 4 Mar 2013; revised 2 Apr 2013; accepted 2 Apr 2013; published 10 Apr 2013

both configurations. Consequently, in the following, all experimental results are discussed in terms of the pump fluence (energy density).

For each laser, the power transfer function and spectra were measured. The threshold given in the text for each laser is obtained by averaging measurements taken at different closely-spaced positions on a device. In order to determine the operating lifetime, the intensity of each laser was monitored and recorded every thirty seconds (i.e. every ~300 pulses) while operated above threshold at a pump fluence of 3.5 mJ/cm$^2$ unless stated otherwise in the text. This represents a fluence 30 to 100 times the threshold depending on the type of lasers. Results were then plotted versus the number of pulses. The resulting operation lifetimes are given in terms of the pump energy fluence ($F_{deg}$) a device has been exposed to when its output intensity falls to 1/e of its initial value. Lasers were characterised in air and ambient conditions except in a few instances, specified in the text, when the lasers were immersed in DI water.

*3.2. Mode profile*

For the discussion on the threshold performance in section 4, the laser mode transverse intensity profile and its overlap with the gain region were calculated for the different types of lasers. This overlap, characterised by the overlap factor as defined further, is important because it influences the modal gain and hence the laser threshold (a higher overlap factor leading to a lower threshold in principle). The calculations were made by considering slab waveguides equivalent to the laser structures, i.e. with the appropriate refractive indices and thicknesses, and using a multilayer matrix model in order to determine the $TE_0$ intensity profile across the whole laser structure [32]. In the case of neat and nanocomposite lasers there is only one layer to be considered, the gain material T3 or the polyimide nanocomposite, enclosed between a semi-infinite epoxy substrate (NOA65) and air or water. For encapsulated devices an additional layer representing the PVA (refractive index~1.55) was taken into account. The effective index for the TE0 mode was first determined and the mode intensity profile subsequently derived. The overlap factor was deduced from the profile by the relation $\frac{\int_{active\_region} I(z)\cdot dz}{\int_{-\infty}^{+\infty} I(z)\cdot dz}$ where the integral in the numerator is taken over the thickness of the gain region (patterned region in Fig. 2), z is the direction of the stack of layers, i.e. the transverse direction of the laser structure, and I(z) is the mode intensity profile. As an example, the mode and refractive index profiles of a neat laser and an encapsulated laser having an 180nm thick PVA layer are plotted in Fig. 2.

#186104 - $15.00 USD Received 4 Mar 2013; revised 2 Apr 2013; accepted 2 Apr 2013; published 10 Apr 2013

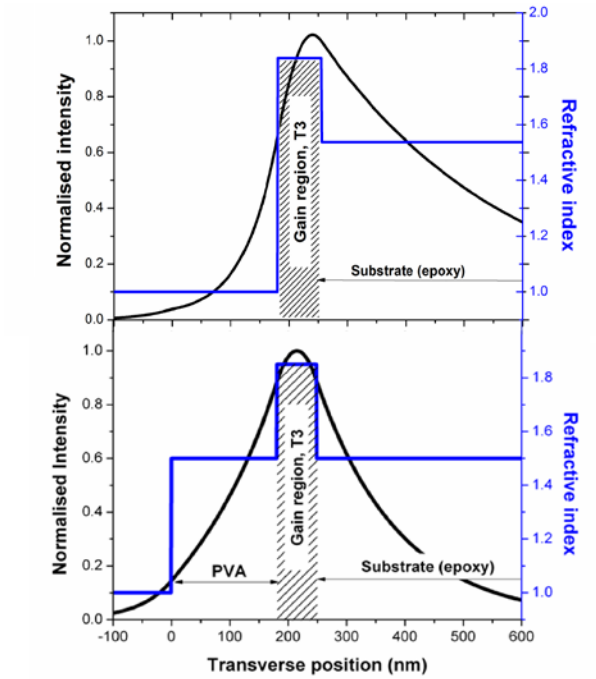


Fig. 2. Mode and refractive index profile of a neat laser (top) and an encapsulated laser (bottom).

## 4. Experimental results and discussion

### *4.1. Neat T3 lasers*

Neat T3 lasers were made and their characteristics measured in order to use them as references for the nanocomposite and encapsulated lasers. Two reference lasers were fabricated using solution of T3 dissolved, respectively, in THF and in toluene to verify the effect of the nature of the solvent on the laser operation lifetime. These two solvents enter in the fabrication of the nanocomposite and encapsulated lasers respectively (see section 2).

The power transfer functions and the spectra of both lasers are plotted in Figs. 3 (a) and 3(b). The T3/THF laser emits at 440.6 nm and the T3/toluene laser emits at 426.3 nm. The wavelength difference is simply attributed to the thickness of the gain region, which is around ~130 nm for the T3/THF sample while it is ~75 nm for the T3/toluene device (see section 2.a). A thinner gain region leads to a shorter wavelength. Average threshold energy fluence, Fth, is found to be 30 ± 3 μJ/cm$^2$ per pulse for the T3/THF laser whereas it is 70 ± 7 μJ/cm$^2$ for the T3/toluene laser. The difference in threshold is again an effect of the thicker T3 layer thickness for the T3/THF laser. The 440.6 nm emission wavelength is better aligned with the T3 spectral gain maximum, which peaks around 435-440nm [32]. Furthermore, the thicker gain region of the T3/THF device leads to a higher spatial overlap factor and hence a higher modal gain. Using the model described in section 3, the calculated overlap factor for the T3/THF laser and T3/toluene laser are found to be respectively 16.7% and 12.5%. Such values are consistent with the lower threshold for the laser having the thicker gain region.

The intensity decay of the neat T3/THF device was measured for 15 minutes (9000 pulses) and the intensity plotted against the number of pulses (Fig. 3(c)). A mono-exponential decay is fitted to the curve, giving a 1/e degradation dosage, Fdeg, of 9.4 ± 2.5 J/cm$^2$. Neat T3/toluene lasers have a similar Fdeg (11.5 ± 5.8 J/cm$^2$) [8]. This means that the use of either THF or toluene as solvent has no significant effect on the degradation dosage of T3 and

#186104 - $15.00 USD Received 4 Mar 2013; revised 2 Apr 2013; accepted 2 Apr 2013; published 10 Apr 2013

therefore the degradation characteristics of devices fabricated with these solvents can be directly compared.

The intensity decay of the neat laser was also measured in water (Fig. 3(c)). This was done for two reasons: (i) to study the operation of the organic laser when immersed in a polar solvent, which is relevant for example for biosensing applications and (ii) to measure the degradation of the laser when placed in an oxygen-poor environment, i.e. not in air. The intensity was still recorded every 300 pulses but the device was exposed to a higher pump intensity of 13.8 µJ per pulse (7.6 mJ/cm$^2$, 250 times the threshold). A two-fold improvement in Fdeg is obtained, with 19.5 ± 5.0 J/cm$^2$, compared to operation in air. This improvement is attributed to the fact that less free oxygen molecules are present in water than in air, so the device does not photo-oxidize as fast. It is interesting to note that the emitted wavelength stays constant on the timescale of the measurement even as the laser intensity degrades. This indicates that such lasers can be used for refractive index sensing in solution.

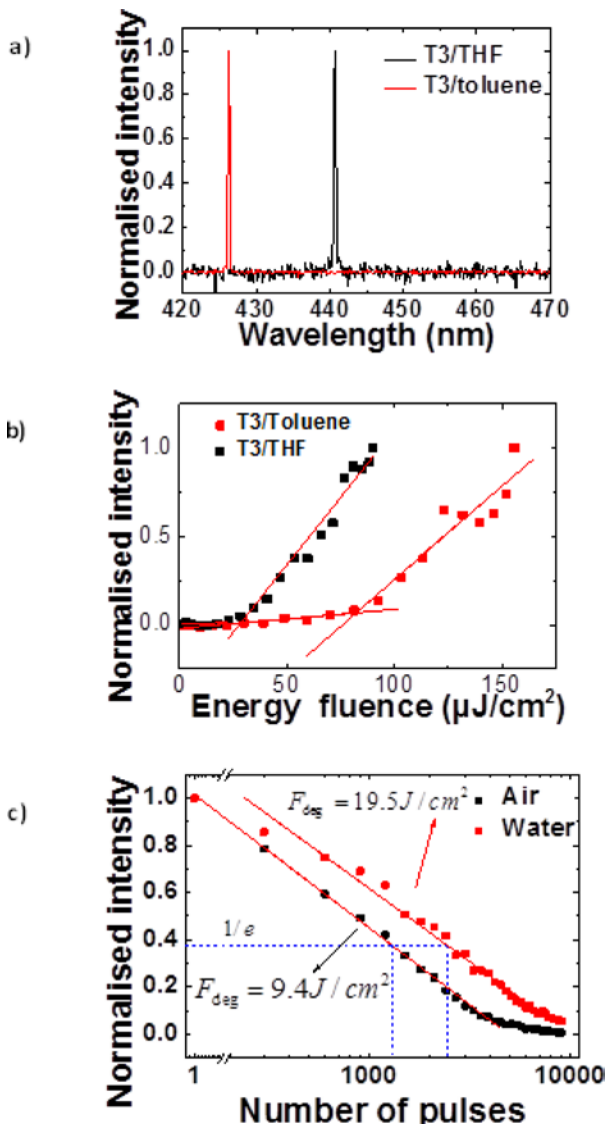


Fig. 3. (a) and (b) Respectively spectra and power transfer functions of a neat T3/THF and T3/toluene lasers, (c) comparison of the intensity decay of a T3/THF in air and water.

#186104 - $15.00 USD Received 4 Mar 2013; revised 2 Apr 2013; accepted 2 Apr 2013; published 10 Apr 2013

*4.2. Nanocomposite lasers*

The characteristics of a typical nanocomposite laser are shown in Fig. 4. It emits at 428.6 nm (Fig. 4(a)) and has a threshold of 115 ± 10 μJ/cm$^2$, which is about 1.6 times the value found for the neat T3/toluene laser emitting close to this wavelength and 3.7 times higher than the T3/THF laser emitting at 440.6 nm (see Fig. 4(a)). The increase in threshold is mainly attributed to residual pump absorption by the matrix at 355 nm and to the slightly lower density of T3 molecules.

Figure 4(b) shows a comparison of the photostability in air of the nanocomposite laser with the neat OS laser. The polyimide nanocomposite brings a ~3-fold improvement in terms of photostability with a Fdeg of 27.0 ± 6.5 J/cm$^2$. The lifetime of another nanocomposite laser was measured both in air and water at a pump energy of 13.8 μJ per pulse (7.6 mJ/cm$^2$, about 70 times threshold). Results are plotted in Fig. 4(c). The intensity decay is found to be the same in both media with a Fdeg of 22.0 ± 4.5 μJ/cm$^2$, whereas it was twice as long in water for the neat T3 laser. This result shows that the CP1-nanocomposite approach slows-down the degradation of the organic semiconductor and that the intensity decay is probably caused by the oxygen already present in the material after the fabrication process (the lasers being made in air). It also indicates that the benefit brought by the nanocomposite in terms of photostability for biosensing applications requiring immersion of the laser in water/solution is only marginal. Nevertheless, it may bring other potential advantages e.g. for surface functionalization.

#186104 - $15.00 USD Received 4 Mar 2013; revised 2 Apr 2013; accepted 2 Apr 2013; published 10 Apr 2013

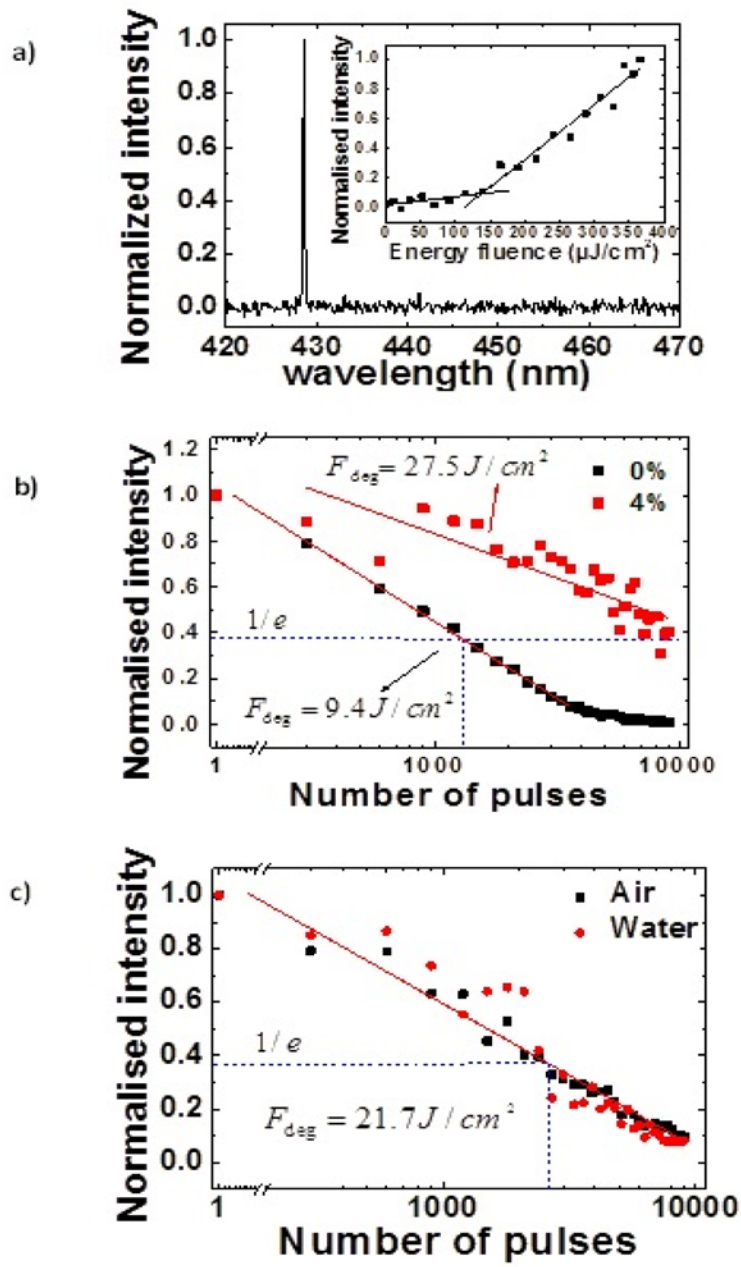


Fig. 4. (a) Emission spectrum and power transfer function of a nanocomposite laser, (b) comparison of the energy decay of the nanocomposite and neat laser, (c) intensity decay of the nanocomposite laser in air and in water.

*4.3. Encapsulated laser*

4.3.1. Laser with a 180nm thick PVA film

The emission wavelength of an encapsulated laser with a 180nm-thick PVA layer is shown in Fig. 5(a) and is 438.9 nm. The average threshold is measured at 25 ± 6 μJ/cm$^2$ (inset of Fig. 5(a)). These values show that the encapsulating layer both redshifts the oscillation wavelength and lowers the threshold when comparing to the equivalent neat laser (Fth~70 ± 7

#186104 - $15.00 USD Received 4 Mar 2013; revised 2 Apr 2013; accepted 2 Apr 2013; published 10 Apr 2013

$\mu J/cm^2$ for a 426.3 nm emission). These effects are mainly due to changes in the refractive index profile of the laser structure as shown in Fig. 2. As a result of the PVA layer addition, the laser mode is pulled away from the substrate and overlaps more with the gain region leading to an increase in the effective refractive index of the mode. To verify this point the modal effective index and the corresponding overlap factor were calculated and found to be 1.543 and 12.5% for the neat laser and 1.5906 and 15.9% for the laser encapsulated with 180 nm of PVA. This is consistent with the emission of a red-shifted wavelength and lower threshold observed experimentally.

The lifetime of the T3/PVA laser was measured and compared to the previous lifetimes obtained for the neat and the nanocomposite devices (see Figs. 5(b) and 5(c)). The intensity of this OS laser stays stable for 13,000 pulses and then starts to decrease slowly. We attribute the initial, stable phase to the time it takes to photooxidise the PVA film when photopumped in air and for the oxygen to migrate to the active region. The second phase characterised by an exponential drop in intensity corresponds to the photodegradation of the organic semiconductor. The 1/e degradation dosage, Fdeg, is here $44.0 \pm 1.5$ $J/cm^2$, i.e. 1.6 times longer than for the nanocomposite laser and 6.2 times longer than for the neat laser. Crucially, and unlike the nanocomposite lasers, this increase in lifetime is accompanied with a reduction in the threshold fluence.

#186104 - $15.00 USD Received 4 Mar 2013; revised 2 Apr 2013; accepted 2 Apr 2013; published 10 Apr 2013

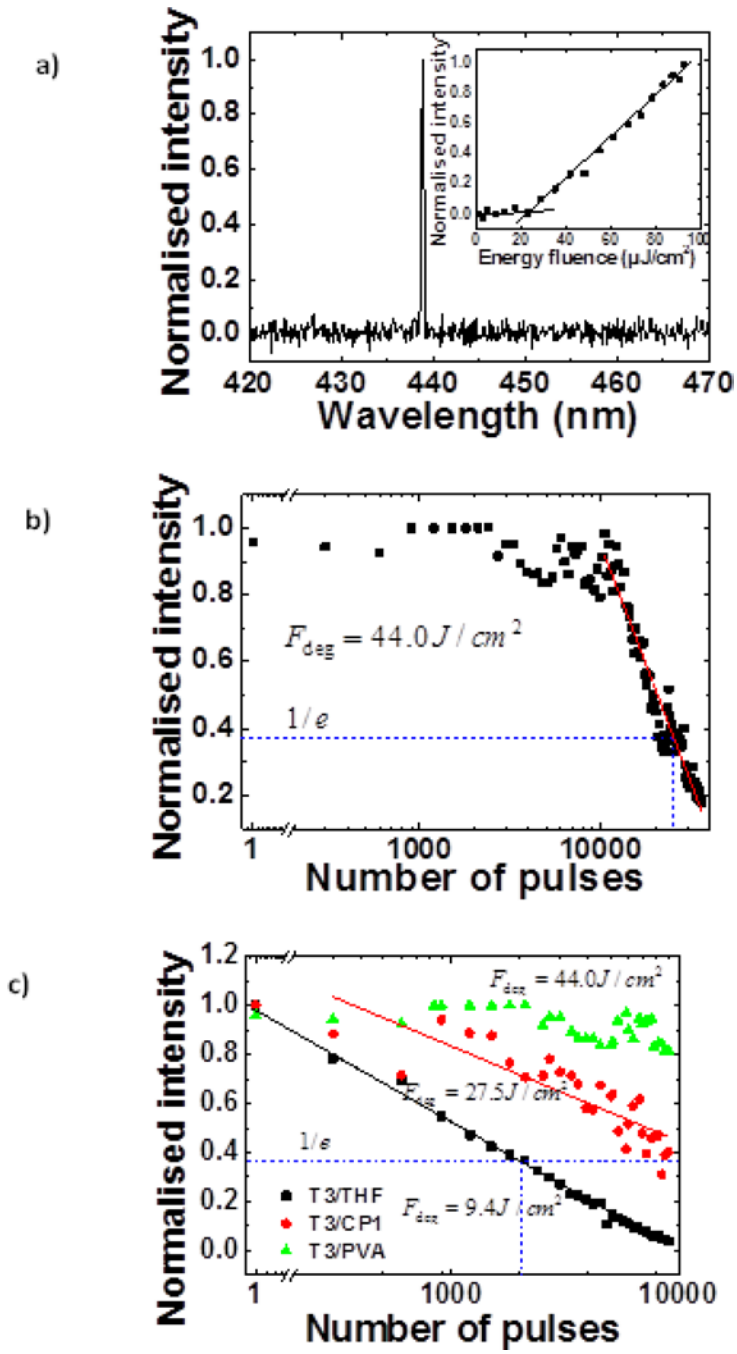


Fig. 5. (a) Spectrum and power transfer function of an encapsulated laser with a 180nm PVA layer, (b) intensity decay of the encapsulated laser, (c) comparison of intensity decay of the encapsulated laser with the nanocomposite laser and the neat laser.

4.3.2. Laser with a 580nm thick PVA film

The thickness of the encapsulating film was increased to 580 ± 70 nm in order to study the influence on the laser photostability.

#186104 - $15.00 USD Received 4 Mar 2013; revised 2 Apr 2013; accepted 2 Apr 2013; published 10 Apr 2013

The emission wavelength of the device shown in Fig. 6(a) is at 440.9 nm. The further 2nm red-shifted emission with respect to the previous device mainly results from the higher effective index of the laser mode induced by the thicker PVA film (1.5875 versus 1.5832 as determined with the multilayer model). The average threshold fluence is measured to be 36 ± 8 μJ/cm$^2$, i.e. not significantly higher (Fig. 6(a)).

A hundred times above threshold the laser intensity of the sample was stable for 79,400 pulses (equivalent to 132 minutes at 10Hz operation). To accelerate the degradation the frequency of the pulses was increased to 14 Hz after 50,700 pulses. After the 79, 400-pulse-long plateau, the laser intensity started to decay. The pump energy fluence for degradation Fdeg is found to be 280 ± 20 J/cm$^2$, which is ~6.5 times higher than for the thinner encapsulated laser (Fig. 6(b)) and 40 times higher than for the neat T3 laser. The dominant degradation is assumed here to come from molecular oxygen diffusing from the environment into the gain layer. The improvement in operation lifetime is attributed to the thicker PVA film offering a better oxygen barrier. Basically, it takes longer for the PVA to degrade and for oxygen to reach the gain material. Results also indicate that the amount of molecular oxygen trapped in the OS after fabrication is lower than in the case of the nanocomposite lasers. To the best of our knowledge, this value of Fdeg is the highest reported for a mechanically-flexible organic laser [8,33,34]. Importantly, it is achieved with no trade-off on the threshold performance.

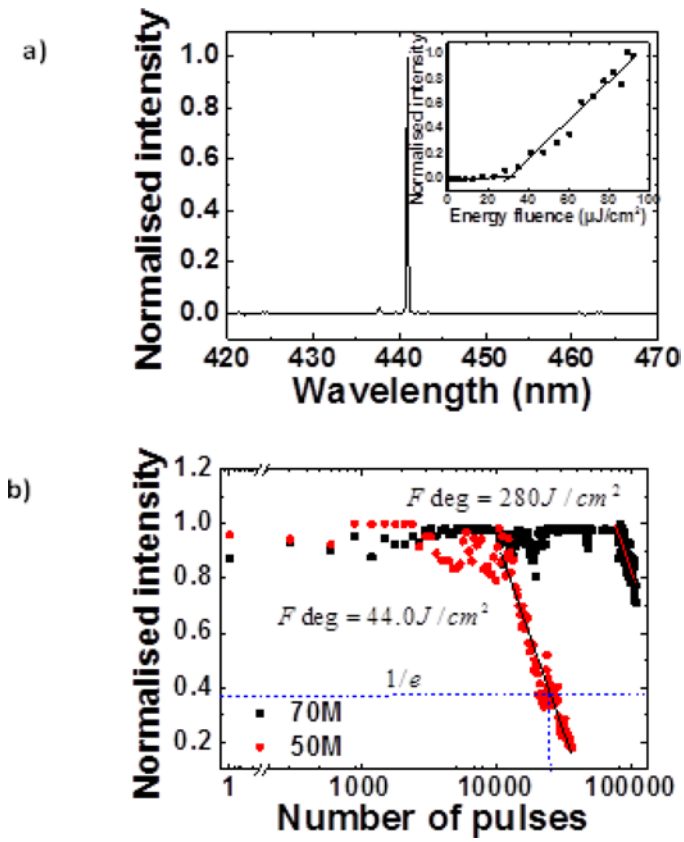


Fig. 6. (a) Emission spectrum and power transfer function of the encapsulated laser with a 580nm-thick PVA layer, (b) comparison of the energy decay of both encapsulated lasers.

#186104 - $15.00 USD Received 4 Mar 2013; revised 2 Apr 2013; accepted 2 Apr 2013; published 10 Apr 2013

## 5. Conclusion

The operating lifetime under ambient conditions of mechanically-flexible organic semiconductor lasers based on monodisperse star-shaped oligofluorenes has been improved by using two approaches. A flexible organic laser comprising a T3-polyimide nanocomposite showed a ~3-fold photostability improvement in air over an equivalent neat OS laser, albeit with an increase in threshold up to 115 ± 10 μJ/cm$^2$. A flexible OS laser encapsulated with an oxygen barrier polymer (PVA) showed a photostability improvement of ~40 combined with an improvement in the threshold performance. In conclusion, we have managed to encapsulate a mechanically flexible OS laser with a thin polymeric film and demonstrated improved operation stability in air for a total degradation dosage of 280.0 ± 20 J/cm$^2$. The latter is, to our knowledge, the highest reported for a mechanically-flexible organic laser and corresponds to a working lifetime of about 7 hours under 10Hz pulse-pumping before the intensity falls to 1/e of its initial value. The structure has also the benefit of lowering the device threshold to 36 ± 8 μJ/cm$^2$ by rendering the laser refractive index profile more symmetric. Table 1 summarises the main results of this study.

**Table 1. Summary of the Results on Nanocomposite and Encapsulated Lasers**

| Type of OS laser | | Air | | | Water |
|---|---|---|---|---|---|
| | | **Threshold μJ/cm$^2$** | **Degradation fluence J/cm$^2$** | **Wavelength (nm)** | **Degradation fluence J/cm$^2$** |
| **Neat** | **T3/toluene** | 70 ± 7 | 11.5 ± 5.8 [8] | 440.6 | x |
| | **T3/THF** | 30 ± 3 | 9.4 ± 2.5 | 426.3 | 19.5 |
| **Nanocomposite** | **T3/CP1 (4%)** | 115 ± 10 | 22.0 ± 4.5-27.0 ± 6.5 | 428.6 | 22.0-27.5 |
| **Encapsulated** | **180nm-thick PVA** | 25 ± 6 | 44 ± 1.5 | 438.9 | x |
| | **580nm-thick PVA** | 36 ± 8 | 280 ± 20 | 440.9 | x |


## Acknowledgments

The authors would like to thank the Engineering and Physical Sciences Research Council for funding under the grant EP/F05999X/1, HYPIX, Hybrid organic semiconductor/gallium nitride/CMOS smart pixel arrays and the grant EP/J021962/1, Hybrid Colloidal Quantum Dot Lasers for Conformable Photonics.



#186104 - $15.00 USD Received 4 Mar 2013; revised 2 Apr 2013; accepted 2 Apr 2013; published 10 Apr 2013